INCREASING THE EFFICIENCY OF ROTOR-ONLY AXIAL FANS WITH CONTROLLED VORTEX DESIGN BLADES

Massimo MASI[1], Stefano CASTEGNARO[2], Andrea LAZZARETTO[2]

[1] *University of Padova. Department of Management and Engineering - DTG, stradella S. Nicola, 3. 36100 Vicenza, Italy*

[2] *University of Padova. Department of Industrial Engineering - DII, via Venezia, 1. 35131 Padova, Italy*

SUMMARY

A design criterion aimed at increasing efficiency without reducing total pressure of Controlled Vortex Design rotor-only tube-axial fans is introduced. The criterion is applied to a production axial fan featuring a 0.44 hub-to-tip ratio and an almost constant swirl velocity distribution at the rotor outlet. In particular, the efficiency improvement is attempted for a fan size characterised by a quite low blade Reynolds number. The criterion is exploited performing experimental tests on each rotor defined by the successive steps suggested in the design guidelines.

INTRODUCTION

Rotor-only tube-axial fans are commonly used when relatively high flow rates coupled with low-pressure requirements have to be satisfied by simple (i.e., low cost) fan layouts. Disregarding considerations of costs, statistical data such the meaningful Cordier's diagram (see e.g., [1]) assess that the rotor-only tube-axial layout is a valuable choice in terms of energy efficiency when a quite high fan specific speed is required. This indication is physically justified because the low-pressure requirement can be satisfied by rotor bladings featuring limited outlet swirl component (i.e., negligible/null advantages are obtainable by straightener addition) and because the high flow rate requirement complies with the low hub-to-tip ratio feature which limits the difference between rotor and fan outlet sections (i.e., negligible advantage are obtainable by tail-cone addition) [2]. In fact, Osborne [3] stated at 85% the maximum total efficiency attainable from free-vortex design (FVD) low-pressure tube-axial fans. On the other hand, this fan configuration is commonly employed also in case of low-to-medium pressure requirements, because of motivations which exceeds their

simple layout and low cost. In fact, they are capable of relatively high total pressure rise when equipped with Controlled Vortex Design (CVD) rotor bladings. CVD by the second half of the last century has shown to be attractive for the performance increase of axial-flow rotors [4] especially when blades were originally designed according to the free vortex criterion [5]. In fact, CVD allows to overcome total pressure limitations of low hub-to-tip ratio FVD rotors which unavoidably feature low loaded bladings to avoid the aerodynamic stall of the spanwise blade region close to the rotor hub [6].

During the last fifteen years, the advancements in the knowledge of the effects due to non-radial stacking line of the blade [7] have allowed to improve performance [8] and to reduce noise [9] of tube-axial industrial fans. In a recent work [10] we collected within a sequence of two procedures (which can be performed without using CFD) some design guidelines that allow to increase total pressure of a rotor-only tube axial fan featuring a constant swirl blade design without reduction in total efficiency. The theoretical justification of the procedure aimed at increasing fan total pressure has been reported in [11] where advantages of forward sweep incorporation into CVD rotors are discussed by formalising a fluid-dynamic analogy between blades for low hub-to-tip ratio rotor and swept wings. Previously, a much more detailed procedure which requires the aid of iterative CFD calculations to incorporate forward sweep in CVD rotors has been suggested by Vad [12]. Compared with the original unswept CVD rotor, the experimental data reported in [12] showed an efficiency gain of about 3%, whereas the CFD calculations performed in [10] showed an increases of fan total pressure of about 10% at design point keeping similar values of total efficiency.

However, the efficiency requirements [13] imposed by the new European Directive 2009/125/EC [14] are hardly satisfied by many highly loaded rotor-only axial fans of current production. In this context, researches are developing aimed at finding solutions to increase the efficiency of low-speed axial flow rotors (see, e.g., [15]). In reference [15], the authors processed an extensive set of literature data and pointed out that the forward sweep of rotor bladings may allow efficiency gain which tends to increase with the spanwise gradient of blade circulation. In particular they observed a maximum total efficiency gain (from 2% to 3%) due to forward sweep addition for CVD rotors, which tends to be minor for FVD rotors.

The paper starts with a discussion of the efficiency losses related with the rotor-only tube-axial fan configuration. The conceptual steps of the design guidelines aimed at increasing fan total pressure suggested in the previous authors'work [10] are here partially re-arranged in order to obtain an increase of total efficiency without reducing the total pressure of low hub-to-tip ratio rotor-only tube-axial fans. These design guidelines are applied to an axial fan featuring a value of 0.44 for the hub-to-tip ratio and an almost constant swirl velocity distribution at rotor outlet. The fan is a 1:2 scaled model of a current industrial machine and features a quite low blade Reynolds number. The reliability of the proposed methodology is exploited performing experimental tests.

EFFICIENCY LOSSES IN ROTOR-ONLY TUBE-AXIAL FANS

The most complex layout of a single stage industrial axial-flow fan is composed by four main components: an axial tube, which is the fan casing, a stationary pre-swirler blading (sometime preceded by the electric motor and related struts), the fan rotor, and a stationary straightener. These components may be preceded by a bell-mouth inlet flanked to the tube to limit inlet pressure losses and followed by a tail cone to limit diffusion losses downstream from the last blade row. The electric motor is usually located upstream from all the blade rows to be efficiently cooled by the free air flow. However, fan layouts in which the motor is incorporated within the fan hub or follows the last blade row or is located outside the tube are used as well.

Given an industrial fan of diameter size D which features total pressure rise pt at flow rate Q_v while operating with air at mass density ρ and rotor angular speed ω, its actual total pressure coefficient $\Psi = (pt/\rho)/(\omega D)^2$, can be conceptually split in the following three terms:

$$\Psi = \Psi_{rot} - \Delta\Psi_v (1-\eta_D) - \Delta\Psi_\varepsilon (1-\eta_S) \tag{1}$$

where Ψ_{rot} is the rotor total pressure coefficient, $\Delta\Psi_v$ is the dimensionless difference between the mean axial component of the dynamic pressure at rotor outlet and the dynamic pressure at fan outlet (by convention uniform and purely axial), and $\Delta\Psi_\varepsilon$ is the dimensionless difference between the mean swirl component of the dynamic pressure at rotor outlet and fan outlet (null by convention).

In case of negligible inlet losses, eq.(1) is valid for all single stage fan configurations except the one including stationary pre-swirler. Thus, eq.(1) clearly states that the amount of dynamic pressure theoretically recoverable downstream from the rotor as static pressure is related to the downstream diffuser/tail cone efficiency η_D and the straightener's efficiency η_S.

Given p_{t1} and p_{t2}, which are the total pressures at rotor inlet and outlet respectively, rotor total pressure coefficient (Ψ_{rot}) writes:

$$\Psi_{rot} = \frac{p_{t2} - p_{t1}}{\rho(\omega D)^2} = \Psi^{is}_{rot} * \eta_{aer} \tag{2}$$

Where Ψ^{is}_{rot} is the isentropic (i.e., loss-free) total pressure coefficient, and $\eta_{aer} = P_{aer}/P_m$ is the rotor aeraulic efficiency defined as the ratio between aeraulic power to the air flow ($P_{aer} = (p_{t2} - p_{t1}) Q_v$) and mechanical power at rotor shaft P_m.

According with eq.(2), the dimensionless form of Euler work equation for fans without pre-swirl, after some algebraic manipulations, gives:

$$\Psi_{rot} = \Psi^{is}_{rot} * \eta_{aer} = \frac{2}{\pi} \frac{x_{MR}}{(1-v^2)} \Phi\varepsilon_s \eta_{aer} \tag{3}$$

Where $\Phi = Q_v/(\omega D^3)$ is fan flow rate coefficient, $\varepsilon_s = c_{u2}/c_a$ is the rotor mean swirl coefficient, x_{MR} is the dimensionless mean-radius that gives the same rotor work ideally acting on the whole flow rate at mean axial velocity component (c_a), and v is the hub-to-tip ratio.

Similarly, the dimensionless parameters $\Delta\Psi_v$, and $\Delta\Psi_\varepsilon$ write:

$$\Delta\Psi_v = (\frac{2}{\pi}\frac{\Phi}{1-v^2})^2 \, 2v^2(2-v^2) \tag{4}$$

$$\Delta\Psi_\varepsilon = (\frac{2}{\pi}\frac{\Phi}{1-v^2})^2 \, 2\varepsilon_s^2 \tag{5}$$

The following general expression of fan without pre-swirler total efficiency $\eta_T = Q_v \, pt / P_m$ can be obtained by substituting eqs.(3)-to-(5) in eq.(1) and then dividing the resulting equation by Ψ^{is}_{rot}.

$$\eta_T = \eta_{aer} - (\frac{2}{\pi}\frac{\Phi}{1-v^2})\frac{2v^2(2-v^2)}{x_{MR}\,\varepsilon_S}(1-\eta_D) \; - \; (\frac{2}{\pi}\frac{\Phi}{1-v^2})\frac{2\varepsilon_S}{x_{MR}}(1-\eta_S) \tag{6}$$

Considering now the simplest rotor-only tube-axial fan layout (i.e., without tail-cone) and assuming no natural recover of dynamic pressure (i.e., $\eta_D = \eta_S = 0$), the ideal fan total efficiency (i.e., loss-free theoretical efficiency) becomes:

$$\eta_T = 1 - (\frac{2}{\pi}\frac{\Phi}{1-v^2})\frac{2v^2(2-v^2)}{x_{MR}\,\varepsilon_S} - (\frac{2}{\pi}\frac{\Phi}{1-v^2})\frac{2\varepsilon_S}{x_{MR}} \tag{7}$$

Eq.(7) clearly quantifies the well-known and unavoidable efficiency penalisation of the rotor-only tube-axial fan layout. In fact, outside from very low pressure requirements, theoretical fan total efficiency rapidly falls below 85%. Thus, it is expected that actual rotor-only fans often feature a total efficiency lower then 60%, especially for rotor size below 400-500mm, where the additional negative effect due to low Reynolds number plays its role as well.

DESIGN CRITERION TO INCREASE EFFICIENCY

The design guidelines collected in a previous authors' work [10] suggest a first procedure aimed at obtaining a blade design (called here "base" fan blading) which equals total pressure and efficiency of the existing low hub-to-tip ratio fan to be improved but, differently from the existing fan, is well-suited to be modified by a second procedure strictly aimed at increasing the fan total pressure. The latter procedure applied to the constant swirl rotor "base" fan accordingly to the CFD results [10, 14], allowed to: a) increase total pressure rise at the design point of about 2%; b) increase fan total pressure in the whole operation range; c) notably increase fan stall margin at throttling.

These design guidelines can be rearranged in a tool aimed at increasing the efficiency of an existing fan, switching the design point constraint of the final improved solution from keeping the same efficiency to keeping the same total pressure rise.

However, a preliminary analysis of the existing fan must precede the two previously mentioned procedures. Thus, the next three subsections deal with these three distinct procedures.

Analysis of the existing fan

The aim of this analysis performed in three-steps is the estimation of the relevant parameters ε_s, x_{MR}, and η_{aer} of the existing fan rotor (assumed to be a constant swirl rotor).

1.1) Starting from the experimental knowledge of Ψ, Φ and η_T design values and the hub-to-tip ratio ν, the mean-radius swirl coefficient ε_s is obtained by:

$$\varepsilon_s = \frac{\Psi}{\Phi} \frac{\pi(1-\nu^2)}{2\eta_T} \frac{1}{x_{MR}} \qquad (8)$$

where a guess value of the dimensionless mean-radius x_{MR} (e.g., 0.7, [5]) has to be assumed only at the beginning of the iterative procedure.

1.2) Then Eq. (6) must be satisfied by proper estimation of the rotor aeraulic efficiency and tuning of the rotor downstream losses parameters. Note that the natural recovery of static pressure and swirl component at the rotor outlet can conservatively assumed to be null (i.e., $\eta_D = \eta_S = 0$) to obtain a guess value for η_{aer}.

1.3) Finally, the radial equilibrium model suggested in [5] (modified here to deal with constant ε_s CVD rotors) allows to calculate the spanwise axial velocity ratio $\Sigma_a = c_{a2}/c_a$ at rotor outlet by means of the following equations.

$$[\Sigma_a(x)]^2 = [\Sigma_a(x_0)]^2 - 2\varepsilon_s^2 \int_{x_0}^{x} 1/x \, dx + \frac{2}{\phi^2}\left[\eta_{aer}(x) \, x^2 \, \psi(x) - \eta_{aer}(x_0) \, x_0^2 \, \psi(x_0)\right] \qquad (9)$$

$$\frac{2}{1-\nu^2}\int_{\nu}^{1} \Sigma_a(x) \, x \, dx = 1 \qquad (10)$$

Where the terms $x = 2r/D$, x_0, $\psi(x) = 2\varepsilon_s \, c_a /(\omega x D)$, and $\phi = 2c_a /(\omega D)$ are the dimension-less radial coordinate, its specific value at the arbitrarily selected reference location 0, the spanwise distribution of the load factor and, the mean flow factor at rotor inlet, respectively.

The spanwise distribution of the aeraulic efficiency $\eta_{aer}(x)$ in eq.(9) can be assumed uniform and equal to the value provided by the previous step 1.2) to simplify the calculations.

Once the distribution $\Sigma_a(x)$ is known from Eqs. (9-to-10), the rotor total pressure coefficient $\Psi_{ro,}$ is calculated by means of mass-weighted integration of the total pressure distribution in the whole rotor blade span.

Thus, the fan total pressure coefficient required in eq.(8) to improve the estimation of x_{MR} performed at step 1.1), is obtained from eq.(1) after substitution of eqs.(4-to-5).

Steps 1.1) to 1.3) require very few iterations to reach convergence on design x_{MR} (and ε_s and η_{aer}) for the existing fan.

Base fan design

The procedure described herein is aimed at obtaining a blade design, named "base", which:

   a) reaches total efficiency higher than the existing fan to be improved;

   b) is well-suited to be modified by using the design improvement procedure described in the next subsection.

Note that the design improvement procedure of item b) yields a new fan which features higher total pressure while keeps total efficiency of the existing fan, as seen in [10]. Therefore, the higher efficiency aim declared in item a) is expected to be achieved (at unchanged aerodynamic design level) as natural consequence of an overall aerodynamic unload of the "base" fan blading. In other words, the base fan design conceptually pays the total efficiency gain with a total pressure decrease. Thus, the magnitude of the efficiency gain is strictly related to the magnitude of the total pressure increase achievable by implementation of the procedure for design improvement. On the other hand, a change of the aerodynamic design level (see, e.g., the adoption of more efficient airfoil sections) should be an additional efficiency gain featured by the final solution.

As will be explained in the following, the rotor blades of the "base" fan are designed by radial stacking of a specific airfoil section of constant chord, thickness and camber line, and proper spanwise distribution of stagger angle (ξ). This rather basic blade configuration is sought because it assures that each blade section crossed by the actual stream surfaces features always the same shape and dimension whatever be its spanwise location. In fact, in [10] it is shown that the through flow stream surfaces originated by constant swirl CVD bladings resemble truncated cones featuring more or less the same slope in the major part of the blade height.

The procedure can by collected in the following three steps.

I.1)   A first estimate of the corresponding mean-radius swirl coefficient ε_s is obtained by using Eq.(1) after substitution of Eqs.(3-to-5), where $\Psi, \Phi, \nu,$ are the design parameters of the existing fan, whereas η_D and η_S are known after completion of the previous procedure. According with the explanations given for previous item b), η_{aer} value required by Eq.(3) becomes actually the product of the effective rotor aeraulic efficiency and the total pressure gain factor foreseen as result of the succeeding design improvement procedure.

At procedure beginning, the mean-radius x_{MR} can be assumed equal to that of the existing fan.

I.2)   Then, a blade design which assures constant ε_s along the whole blade span is required. The selected cascade should achieve the highest lift-to-drag ratio during operation with the mean-radius velocity triangles obtained in previous step I.1 (some well-established criteria to perform this task are recalled in [6]). Then, the airfoil section of the cascade selected for the blade mean-radius is employed along the whole blade span, so that the resulting blade features span-wise constant chord (l), camber (θ) and thickness (s). Such a design results in an almost constant distribution of the chord-lift coefficient product ($l\ C_L$) if the spanwise distribution of airfoil stagger and design attack

angles (ξ and α_D, respectively) vary according with local velocity triangles and cascade solidity $\sigma = l\,Z/(\pi x D)$ (where Z is the number of blades). Note that, a constant $l\,C_L$ design in the whole blade span is exploited in [4] and the obtained CVD blading featured roughly constant ε_s distribution along blade span.

I.3) The values of x_{MR} and ε_s resulting from step I.1) and the spanwise distribution $\eta_{aer}(x)$ resulting from step I.2) have to satisfy the same simplified radial flow analysis suggested in the step 1.3 of the previous procedure. In addition, the span-wise distribution of the aeraulic efficiency $\eta_{aer}(x)$ has to comply with the overall rotor aeraulic efficiency value used in step I.1).

Similarly to the previous one, also the present procedure requires few iterations to reach convergence on the base fan design values of the parameters ε_s and x_{MR}.

Eq.(6) can be used to evaluate the theoretical total efficiency η_T achieved by the base fan.

Improved fan design

As stated previously, the improved solution has to recover the performance downgrade expected from the "base" fan design, without loosing the efficiency gain. Thus, this third procedure, is actually aimed at increasing the performance of the "base" fan just like the procedure presented in [10], which is summarised in the flow chart showed in Fig.1. The figure shows also the schematic of the blade resulting from the completion of each procedure step.

The sketch of the fan blade named "f" at "design" column in Fig.1, shows the "base" fan geometry obtained after completion of the procedure described in the previous sub-section.
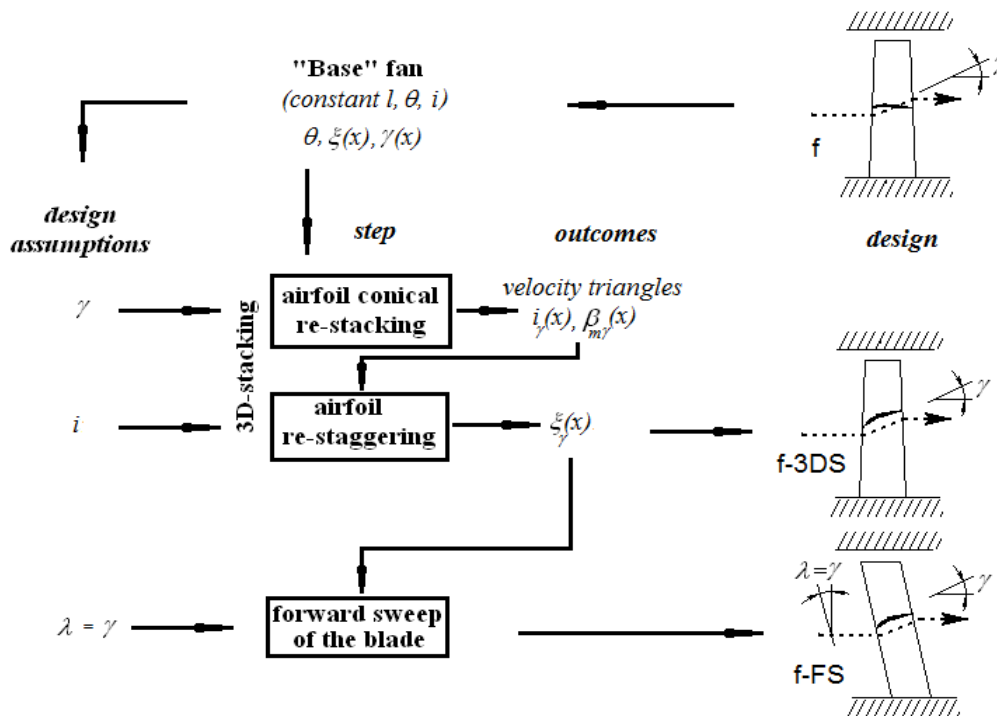

Figure 1: Flow chart of the "improved fan design" procedure. The "base" fan(f) becomes the f-3DS fan after 3D-stacking and finally the f-FS fan after rotor blades forward sweep.

The "3D-stacking" is the first step of the "improved fan design" procedure. Its result is sketched as fan "f-3DS" in Fig.1 under "design" column, and it comprises the following two sub-steps.

- The "airfoil conical re-stacking", which provides the re-positioning of each 2D airfoil section of the "base" fan rotor blading along the approximately conical stream surfaces of slope γ originated by the radial migration of the meridional flow due to CVD. Each two-dimensional airfoil is re-

stacked onto the proper conical surface throughout rotation around the tangent to the cylindrical surface at half length point of its chord.

- The "airfoil re-staggering", which corrects the blade geometry to recover the right design attack angle α_D altered because of the change of leading edge radial coordinate of each airfoil section deriving from previous sub-step. This task is performed using the following Eq.(11) to recalculate the spanwise distribution of stagger $\xi(x)$ ([16]).

$$\xi(x) = \beta_1(x) - \alpha_D \tag{11}$$

where $\beta_1(x)$ is the spanwise distribution of the angle between relative velocity and rotor axis at rotor inlet ($\beta_1(x)$ values are taken at the intersection between each conical stream surface and the rotor inlet section).

Note that, the simplified radial flow model (see, previous procedure item 1.3) allows also to calculate the γ angle required for 3D-stacking by using the following equation

$$\gamma = \max\left\{ \arctan\left[\frac{x_{out} - x_{in}}{l_{root} \cos(\xi_{root})} \frac{D}{2} \right] \right\} \tag{12}$$

where x_{in} and x_{out} are the dimensionless radial coordinates of each stream surface at rotor inlet and outlet, respectively.

The procedure is completed by the forward sweep addition performed by roto-translating each blade section along a cylindrical helix until the proper blade sweep is obtained. This task is required to restore the two-dimensional flow features of the cascade data used for blade design. To restore the aerodynamics of a blade conceived for purely cylindrical flow it is necessary to sweep the blade forward by an angle λ equal to γ in any radial coordinate, nullifying the velocity component along the stacking line [10, 11].

CASE STUDY

A rotor-only tube-axial fan derived from an actual industrial fan has been used as case study to exploit the design guidelines previously presented. The shaded view of the fan and the photograph of its CVD rotor are shown in Tab.2 under column "design parameter".

Experimental set-up and prototyping technique

The experimental tests were performed by using the test rig showed in the left side of Fig. 2. The rig features a plenum chamber at the fan inlet and free delivery, and complies with the standard category-A of ISO-5801 standard on industrial fans test methods and acceptance conditions [17]. Fan volume flow rate is evaluated using suitable orifice plates, stagnation pressure is acquired in the plenum chamber. Static pressure measurements at plenum chamber and orifice plate tappings are taken using water micro-manometers. Table 1 shows the absolute accuracy of the main instruments.

Fan performance are evaluated through the dimensionless parameters fan flow rate coefficient Φ, fan total pressure coefficient Ψ, and fan total efficiency η_T. The fan total pressure curve (Φ - Ψ curve) is strictly compliant with the standards, whereas the efficiency was indirectly obtained by the measurements of motor shaft torque. In fact, the motor is mounted on a swinging chassis which is part of the specifically designed torsion balance (see, the device on the right side of Fig. 2).

Figure 2:The ISO 5801 category A fan test rig (on the left) and the torsion balance (on the right) used for the experimental tests

All test have been conducted, when possible, at a rotational speed of 1350 rpm. However, the auxiliary fan was unable to overcome the pressure losses in the airway at high flow rates and required the gradual reduction of the tested fan rotational speed up to about 850 rpm. The similarity of operations was therefore not actually met in the higher flow rates test points. In order to account for this, the efficiency data was corrected by using the classical formula of Carter (see, e.g., [18]). As a consequence, and considering also that the power absorption measurements are not compliant with the standards, the actual fan efficiency magnitude could be slightly different from that showed here. However, these data are considered to be accurate enough for a reliable comparison of different designs in terms of efficiency trend and relative magnitude.

Table 1: Main instruments absolute accuracy

Instruments	Accuracy
Water micromanometers	± 0.01 mm H_2O
Rpm counter	± 2 rpm
Torsion balance	± 8.1 N x mm
Wet-dry bulb thermometer	± 1 K
Digital barometer	± 100 Pa
Digital thermometer	± 0.1 K

All the fan rotors experimentally tested feature the same die-casting aluminium alloy hub. This latter is originated by coupling two equal half barrel-like parts which clamp the rotor blades. The rotor blades have been manufactured using the 3D printing Fused Deposition Modeling (FDM) technique. This rapid prototyping tool re-builds the CAD drawing through the deposition of a fused polymer wire (ABS) along succeeding plane paths provided by the CAM software. The adjacent wires melt together originating the final shape. The lower dimension is limited by the diameter of the nozzle which ejects the fused material (0.2 mm in the present case).

Exploitation of the design guidelines

The fan selected for the implementation of the presented procedure aimed at increasing the efficiency is a 1:2 scale model of an industrial rotor-only tube axial fan featuring external diameter equal to 630 mm and total pressure coefficient equal to 0.0202, flow-rate coefficient equal to 0.088 and a quite high peak total efficiency (about 0.64). A reverse engineering analysis process suggested that the blades are likely to be constituted by envelopes of thick cambered plates sections with rounded leading and trailing edges and progressive trailing edge thinning, like those described in [6]. Tab. 2 reports the other main features of the scaled model fan and the photograph of its rotor blade (see, "Model" column). Black markers in Figure 3 show total pressure coefficient and efficiency measured for this fan (Model) at three different values of the blade positioning angle ($\phi_p = 23°$ is the design positioning angle).

The design condition performance obtained from the tests performed on the scale model (see Fig.3) allows to calculate the swirl coefficient ε_s, and the dimensionless mean-radius x_{MR} by using the "analysis of the existing fan" procedure. They resulted equal to 0.648 and 0.756 respectively.

The peak efficiency measured for the scale model (0.59) is notably lower than the peak efficiency featured by the actual industrial fan (0.64). This difference is mainly due to the low blade sections Reynolds number of the scale model which varies from $2x10^4$ to $9x10^4$. The low Reynolds number and the relevant magnitude of blade tip clearance (~2.5% of blade height B) suggest the assumption of quite low rotor aeraulic efficiency η_{aer} (0.772 against the reference value 0.85 recommended in [5] for high blade Reynolds number). This assumption yields an estimation of the natural recovery of static pressure and swirl component at the rotor outlet compliant with $\eta_D = 0.3$ and $\eta_S = 0.075$.

These data are used to perform the "base" fan design procedure aimed at obtaining the spanwise constant chord/airfoil blading of the "f" rotor in Fig. 1. A classic NACA 65810 blade section was selected according with the criterion suggested in [16] for the exploitation of this procedure. Because of the differences in blade airfoil selection (see, columns "f" and "Model" in Tab. 2) a 2% aeraulic efficiency increase ($\eta_{aer} = 0.787$) is assumed for the f rotor. This value has been increased by 1.5% to account for the performance recovery expected by the succeeding "improved fan design" procedure. These assumptions make the "base" fan design procedure converging to a swirl coefficient ε_s equal to 0.619 and a dimensionless mean-radius x_{MR} equal to 0.755. The estimated total efficiency of the final improved fan is equal to 0.617 (i.e., an efficiency gain of about 4.8%), whereas the mass flow averaged value calculated for γ angle according with the simplified radial equilibrium model results equal to 7.5°.

Table 2: Main features of fan under analysis (values assumed/calculated at design condition).

Design parameter	Fan			
	Model	**f**	**f-3DS**	**f-FS**
hub-tip ratio (ν)	0.44			
Blade number Z	10			
blade tip clearance (t_c/B)	~2.5%			
tip solidity (σ)	0.58	0.58	0.58	0.58
blade thickness (s/l)	7%-to-13%	10%		
design swirl coefficient ε_S	≈ 0.65	0.62		
blade airfoil section	cambered plate ($\theta=23°$)	NACA 65810 [16]		
tip stagger angle (ξ)	67°	68.5°	68°	
blade aspect ratio (B/l_{root})	1.55	1.71	1.73	
blade 3D stacking (γ)	0°		7°	
blade sweep (λ)	0°			7°

The knowledge of the f rotor geometrical features and of the meridional through-flow slope γ at design condition allows for the execution of the two steps enclosed in the "improved fan design"

procedure. The columns "f-3DS" and "f-FS" in Tab.2 report the main geometrical features of the intermediate 3D-stacked rotor and the final forward swept rotor respectively.

Results

Diagrams of Figure 3 show total pressure coefficient (on the left side) and total efficiency (on the right side) measured for the existing fan (black markers -"Model" data), the base fan (red markers – "f" data), and the two fans resulting from the execution of the successive steps suggested in the improved fan design procedure, i.e.: the intermediate 3D-stacked fan (blue markers – "f-3DS data) and the final forward swept fan (green markers – "f-FS" data) respectively.

Looking at the design positioning angle data (the two uppermost diagrams), it appears that the "base" f fan total pressure is actually almost equal to the Model fan total pressure in the operation range from design to free delivery, and the Model fan efficiency is not improved differently from what expected. Moreover, both the 3D-stacked rotor and the forward swept rotor perform slightly worse and also reach an unfavourable advance of blade stall. On the other hand, a comparison restricted to these two latter configurations shows that the 3D-stacked fan (f-3DS) features total pressure curve slightly higher than that featured by the forward swept fan (f-FS), whereas the opposite occurs in total efficiency. The f-3DS rotor shows also total pressure slightly higher than f-FS rotor close to stall operation. These two occurrences agree with the better total pressure curve behaviour and worse total efficiency of the f-3DS rotor expected by the simplified theory of blade sweep [11] for low blade aerodynamic load operation.

The scenario is by far more satisfactory at blades positioning angle values higher than design. As expected from the basic statements of the design criterion presented here, the f rotor total pressure at fan best efficiency point is now lower than Model rotor total pressure and the efficiency is increased by percentage values close to the 5% predicted from design calculations. Moreover, the forward swept rotor (f-FS) is capable of maintaining almost unchanged the efficiency gain featured by the base fan (f), differently from the f-3DS configuration which shows efficiency only equal or slightly better than the existing fan configuration (Model). In addition the progressive total pressure increase switching from base (f), to 3D stacked (f-3DS), to forward swept (f-FS) fan configuration confirms the reliability of the procedure aimed at increasing fan total pressure [10-11] which has been rearranged here to the aim of increase fan total efficiency.

An attempt to explain the unsuccessful efficiency gain of the forward swept rotor at design positioning angle resulted from measurements performed in the present case study is twofold:

1) The selection of higher efficiency airfoil sections allows an overall blade unload which, in turn, limits the amplitude of the radial flow migration. If the radial flow is weak, also the advantages descending from sweep incorporation becomes weak.

2) The NACA 65-8-10 airfoil used in all the f, f-3DS, and f-FS blade cascades has been selected here because, according with the experimental database [16], the less cambered NACA 65-4-10 airfoil could have not been sufficient to satisfy design requirements. On the other hand, the NACA 65-8-10 features a quite high camber which performs better at the higher blade loads occurring at higher values of the blade positioning angle.

Finally, it is worth noting that the value of angle $\gamma = \lambda = 7°$ selected to stack the airfoil sections on conical surfaces and to sweep the blade (taken slightly lower then the 7.5° mass flow averaged value calculated by using the simplified radial equilibrium model) is actually a precautionary value. In fact, CFD simulations showed that the maximum angle calculated by a radial equilibrium model for the span-wise distribution of the conical stream surfaces (which results 12.3° in the present case) should be a better value [10].
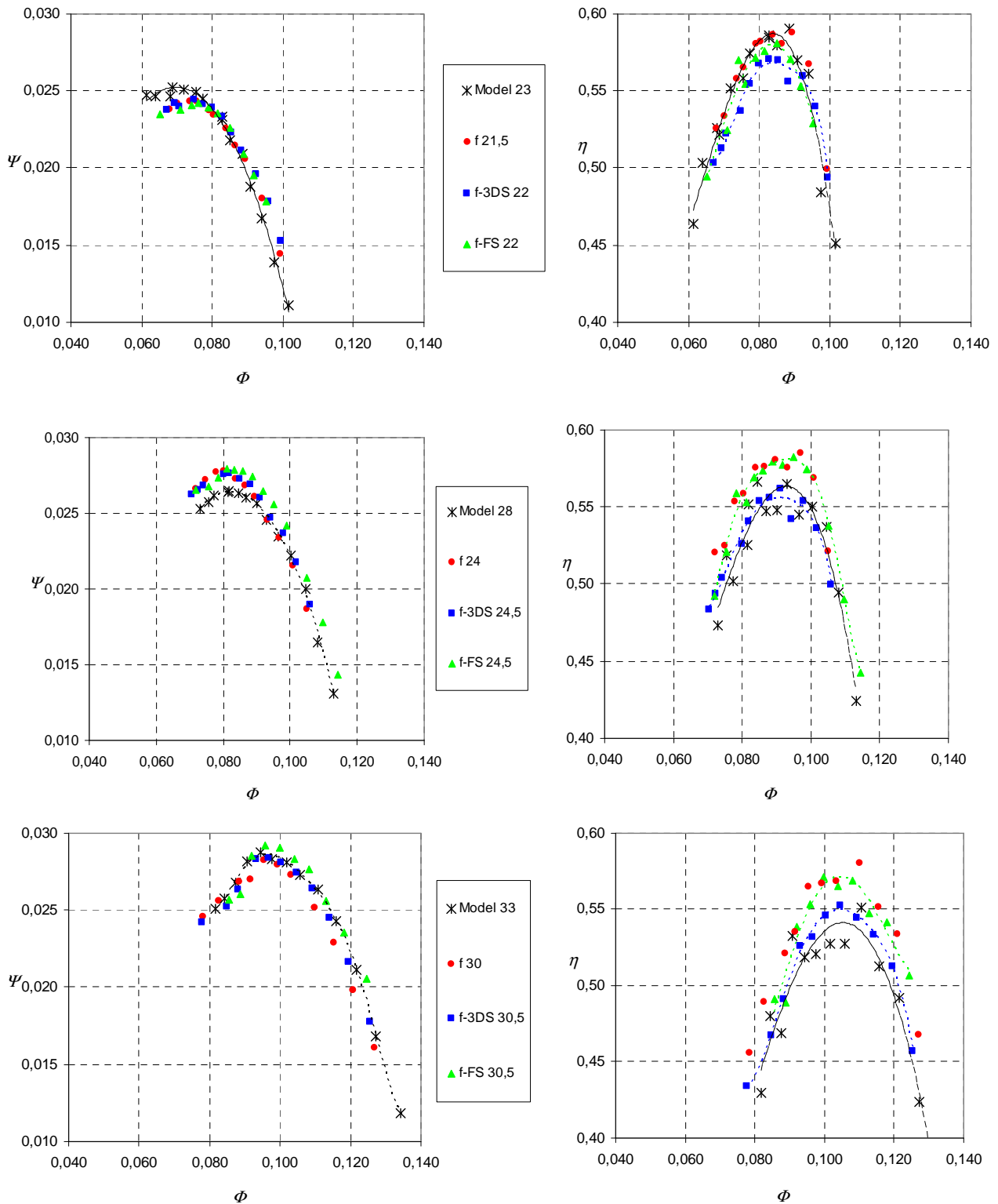
Figure 3:Total pressure coefficient and efficiency of all the tested fans at various blade positioning angle

CONCLUSIONS

Fan total pressure and efficiency measured for each rotor defined by the successive steps of the design guidelines presented here allow to check the reliability of the suggested procedures which are aimed at increasing the efficiency of rotor-only tube axial fans featuring low hub-to-tip ratio. The experimental data show that the design guidelines allowed an increase of peak efficiency up to

5% at blade positioning angles higher than design condition and an extension of the high efficiency operation keeping similar values of the total pressure. On the other hand, the ineffectiveness showed by the suggested procedure at the design value of blade positioning angle requires some improvements/adjustments. A less precautionary selection of blade conical stacking and sweep angle magnitude coupled with a proper increase of chord length in order to restore in the final swept rotor configuration the solidity of the cylindrical cascades designed for the base fan rotor could result in a more satisfactory efficiency gain also at the design value of blade positioning angle.

BIBLIOGRAPHY

[1] R. I. Lewis, *"Turbomachinery performance analysis"*. Arnold, London. **1996**

[2] B. Eck – *"Fans"*. Pergamon Press, Oxford, UK, **1973**

[3] W. C. Osborne – *"Fans"*. Pergamon Press, Oxford, UK, **1966**

[4] A. Kahane – *Investigation of axial-flow fan and compressor rotors designed for three-dimensional flow.* NACA TN-1652, **1948**

[5] R. J. Downie, M. C. Thompson, R. A. Wallis, *An engineering approach to blade designs for low to medium pressure rise rotor-only axial fans.* Experimental Thermal And Fluid Science, 6:376-401, **1993**

[6] R. A. Wallis – *"Axial flow fans and ducts"*. Krieger Publishing Company, Malabar, FL, **1993**

[7] J. Vad – *"Aerodynamic effects of blade sweep and skew in low-speed axial flow rotors at the design flow rate: an overview"*. Proc. IMechE, Part A: J. Power and Energy, 222, 69-85, **2008**

[8] A. Corsini, F. Rispoli – *"Using sweep to extend the stall-free operational range in axial fan rotors"*. Proc. Instn Mech. Engrs, Part A: J. Power and Energy, 218, 129-139, **2004**

[9] M. G. Beiler, T. H. Carolus – *"Computation and measurement of the flow in axial flow fans with skewed blades"*. ASME J. Turbomachinery, 121, 59-66, **1999**

[10] M. Masi, M. Piva, A. Lazzaretto – *"Design guidelines to increase the performance of a rotor-only axial fan with constant-swirl blading"*, ASME paper GT2014-27176, **2014**

[11] M. Masi, A. Lazzaretto – *"A simplified Theory to justify forward sweep in low hub-to-tip ratio axial fan"*, ASME paper GT2015-43029, **2015**

[12] J. Vad – *"Incorporation of forward blade sweep in preliminary controlled vortex design of axial flow rotors"*. Proc. IMechE, Part A: J. Power and Energy, 226, 462-478, **2012**

[13] Regulation of the European Commission (EU) 327/2011 – *Official journal of the European Union - Ecodesign requirements for fans driven by motors with an electric input power between 125W and 500kW*, pp.8-21, **2011**

[14] Directive of the European Parliament and of the Council of the European Union 2009/125/EC – *Official journal of the European Union - Ecodesign requirements for energy-related products,* pp.10-35, **2009**

[15] J. Vad, G. Halàsz, T. Benedek – *"Efficiency gain of low-speed axial flow rotors due to forward sweep"*. Proc. IMechE, Part A: J. Power and Energy, Technical Note 0(0), 1-8, **2014**

[16] C. Emery, L. J. Herrig, J. R. Erwin, A. R. Felix – *" Systematic two-dimensional cascade tests of NACA 65-series compressor blades at low speeds"*. NACA Report 1368, **1958**

[17] ISO 5801 – *Industrial fans - performance testing using standardized airways*, **2008**

[18] A. B. McKenzie – *"Axial flow fans and compressors: aerodynamic design and performance"*. Ashgate, **1997**